

Periodicities in the properties associated with the friction of model self-assembled monolayers

Paul T. Mikulski and Judith A. Harrison*

Department of Chemistry, United States Naval Academy, Annapolis, MD 21402, USA

The classical molecular dynamics simulations presented here examine the periodicities associated with the sliding of a diamond counterface across a monolayer of hydrocarbon chains that are covalently bound to a diamond substrate. Periodicities observed in a number of system quantities are a result of the tight packing of the monolayer and the commensurate structure of the diamond counterface. The packing and commensurability of the system force synchronized motion of the chains during sliding contact. This implies that the size of the simulations for this special case can be reduced so that the simulations can be conducted with sliding speeds and time durations that may bridge the gap between theory and experiment.

KEY WORDS: friction; molecular dynamics; alkane monolayers; self-assembled; monolayers; energy dissipation; atomic force microscopy

1. Introduction

Elucidating the role of monolayer thick lubricants is critical to the development of modern nanoscale technologies, such as magnetic storage devices [1–3] and microelectromechanical systems [4,5]. Adhesion of the molecules to the substrate and good wear resistance are of paramount importance if a material is to be a viable boundary-layer lubricant in these applications. Thus, molecules that are covalently bonded to the substrate, such as those formed from self-assembly, are better candidates for boundary-layer lubricants than Langmuir–Blodgett (LB) films. Therefore, the molecular structure, mechanical properties, and tribological properties of self-assembled monolayer (SAM) materials have been studied a great deal using scanning probe microscopies [6–15].

A number of groups have examined the friction and wear properties of alkanethiols on Au and alkylsilane monolayers on both silicon and mica using the atomic force microscope (AFM) [6,7,9,11–14]. Molecular dynamics (MD) simulations, using the united-atom method, have been used to examine the structure [16–19] and compression of *n*-alkanethiols on Au [20,21], as well as the friction of organic monolayers [22–26]. More recently, SAM materials have been modeled using alkane monolayers [27–29] and the friction and response to compression investigated using MD and a newly developed, reactive hydrocarbon potential [30].

The work presented here uses MD simulations to examine in detail the long-time behavior of a compressed alkane monolayer under shear. A C₁₃ *n*-alkane monolayer is compressed with a commensurate hydrogen-terminated diamond counterface. The effects of the commensurate countersurface and sliding on chain structure, chain motion, and energy dissipation are examined.

* To whom correspondence should be addressed.

2. Experimental

The simulation system consists of 36, *n*-alkane chains covalently bound to the (111) face of a diamond substrate in a (2 × 2) arrangement. The alkane chains are 13 carbon atoms long and the dihedral angles within the carbon backbone are initially in the *anti* configuration (180°). This arrangement of chains was selected because it yields approximately the same packing density and cant as monolayers of alkanethiols on Au(111) [9,31]. The diamond substrate, to which the chains are attached, is composed of seven layers of carbon atoms that contain 144 carbon atoms each. The computational cell in the plane that contains the alkane chains is approximately 30.5 by 26.4 Å (or 22.4 Å²/monomer). The counterface (or tip) is a hydrogen-terminated (111) face of a diamond lattice composed of eight layers that contain 144 atoms each (figure 1).

After the system energy and temperature reach their steady-state values, simulations are performed by holding the bottom layer of the diamond substrate rigid (figure 1(a)). Moving upward from the bottom, the next two layers of the diamond are maintained at a constant temperature of 300 K using generalized Langevin dynamics to simulate coupling with an external heat bath [32]. The remaining diamond layers and the hydrocarbon chains are free to move according to classical dynamics. The equations of motion for all non-rigid atoms are integrated using the velocity Verlet algorithm with a constant step size of 0.25 fs [33]. An infinite interface is simulated by applying periodic boundary conditions in the plane containing the alkane chains.

The potential governing atomic motions is the recently developed adaptive intermolecular reactive empirical bond-order (AIREBO) potential [30]. This potential introduces non-bonded interactions to the REBO potential [34,35], via

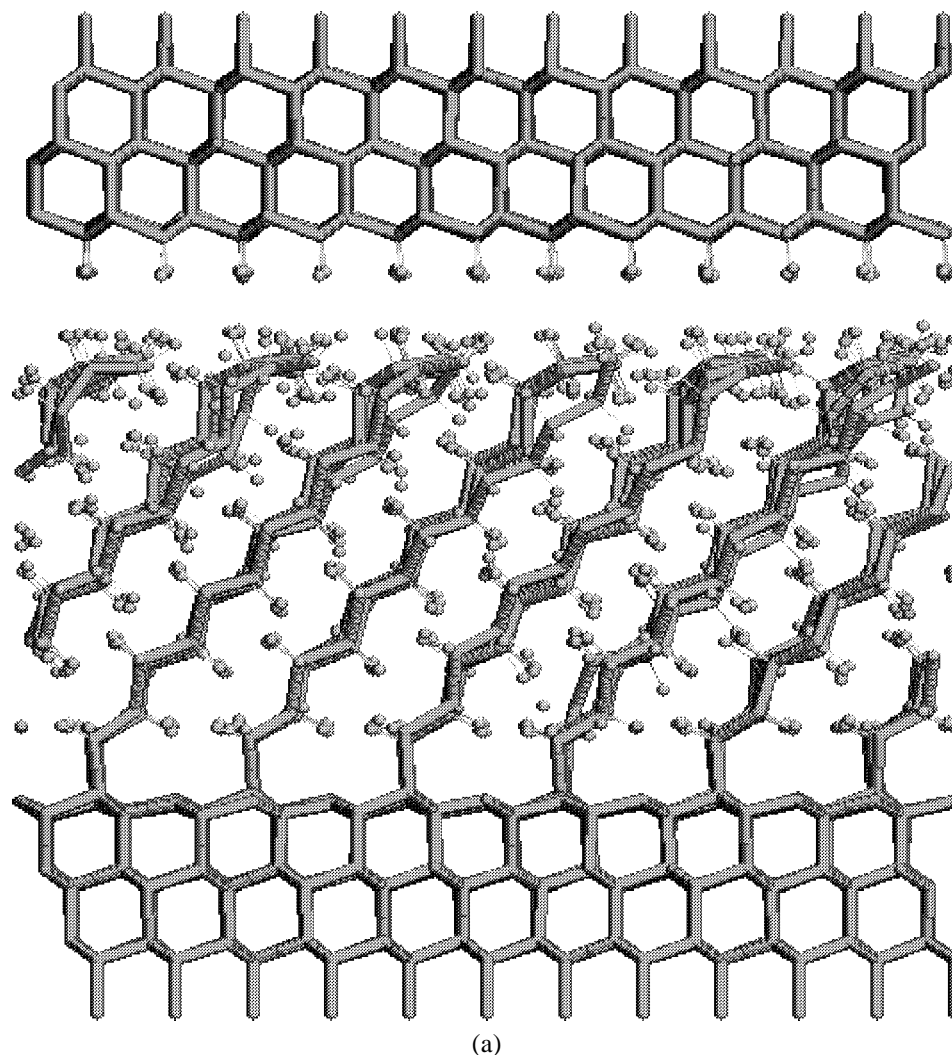


Figure 1. Snapshot of the simulation system after sliding for approximately 6.9 \AA with a normal load of approximately 64 nN ($\sim 8.0 \text{ GPa}$). Carbon atoms are represented in a wireframe format and hydrogen atoms as small spheres. In panel (a) the positive x direction points out of the page and the positive y direction is from left to right. The countersurface is moved in the positive y direction to simulate sliding. The positive z direction completes the right-handed coordinate system. In panel (b) the figure in panel (a) has been rotated 90° so that the positive x direction is from right to left.

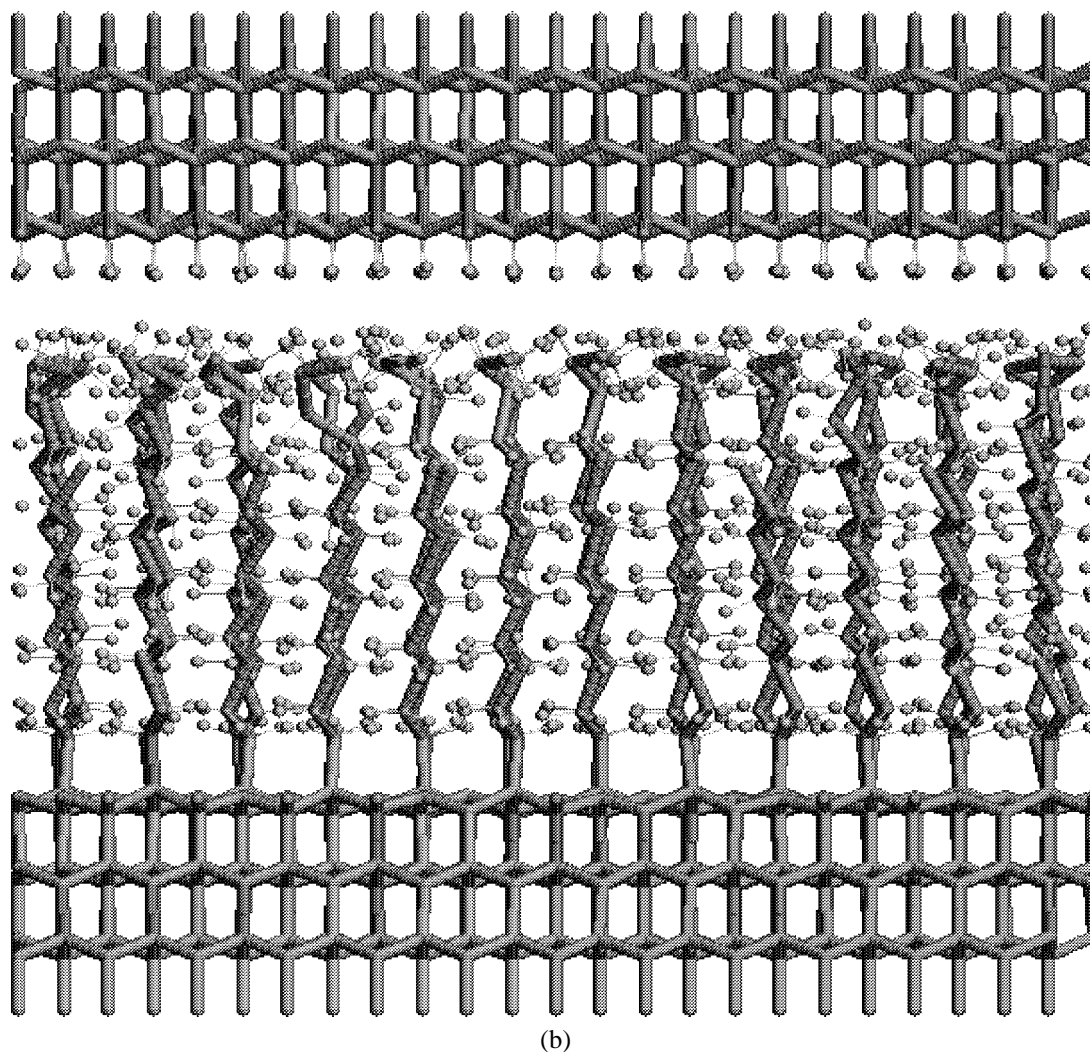
a novel adaptive algorithm, while preserving the chemical reactivity of the original potential. Given the success of the REBO potential in modeling a number of phenomena [36–38], the majority of its covalent bonding parameters were preserved in the AIREBO potential. Thus, because chemical reactions are possible in these simulations, events such as wear and tribochemistry within the alkane-chain films are possible.

During the compression phase, the atoms in the diamond counterface are partitioned in much the same way as the atoms in the substrate. The top layer of atoms is held rigid, an independent Langevin thermostat is applied to the next two layers of atoms, and the remaining layers act under no constraints whatsoever. Compression of the hydrocarbon monolayers is accomplished by moving all rigid atoms in the upper countersurface at a constant velocity of 100 m/s toward the monolayer surface.

Before the commencement of sliding, the downward motion of the countersurface is halted and the system is allowed

to equilibrate for 13 ps . (Moving the countersurface closer to the monolayer increases the applied load on the monolayer.) During the slide, all atoms in the counterface are held rigid and moved with a constant velocity of 50 m/s . This simplifying constraint allows for a cleaner examination of the periodic structure associated with the chain motion. Qualitatively, the difference between this and the more relaxed scenario, which holds only the upper-two layers of the counterface rigid, is small considering that the counterface is much harder than the top portion of the alkane monolayer.

There is evidence that for loads larger than a critical load of approximately 130 nN , the system exhibits qualitatively different behavior owing to the highly constrained volume associated with large loads. That is, it is very difficult to change the conformation of the system due to the compact nature of the chains. In the work described here, a configuration with a normal load of approximately 64 nN ($\sim 8.0 \text{ GPa}$), well below the onset of the constrained volume regime, is selected for sliding. Figure 1 shows a snapshot of the en-



(b)

Figure 1. (Continued.)

ture system during the sliding phase. The direction of sliding (positive y) is along the tilt of the chains, as shown in figure 1(a). A view of the lateral direction is shown in figure 1(b).

The sliding speed of 50 m/s is many orders of magnitude greater than the 10^{-8} m/s speeds typically used in nanoindentation experiments [8,12] and still several orders of magnitude greater than the 10^{-1} m/s speeds commonly used in AFM tapping mode. Simulating a system with long-range intermolecular interactions for long sliding times requires a significant amount of computer time. These constraints restrict the sliding speed to be in the range of 10–100 m/s. Even at 50 m/s, there was adequate time for thermal equilibration of the simulation system. Simulations conducted at speeds of 100 m/s show qualitatively similar behavior for system properties such as force as a function of penetration depth [27,29]. However, gauche defect formation does depend upon the indentation and sliding speed. A slower speed during the compression phase may result in a higher degree of order in the chains relative to one another.

3. Results and discussion

The following discussion will center around plots of various system properties as a function of sliding distance of the counterface. For the sake of clarity, the distance of sliding is expressed in units of the cell length in the sliding direction. The unit-cell length in the sliding direction (approximately 8.8 \AA) is that of the chains which are packed in a (2×2) arrangement. Prior to compression, the entire system is invariant under a translation of the (1×1) unit cell of the counterface. This symmetry is broken in the lateral direction upon compression of the monolayer. This breaking of symmetry modifies the motion of the chains during the sliding phase such that the natural period of the system is over the (2×2) unit cell of the chains. Hereafter, any reference to a unit cell corresponds to the (2×2) geometry of the chains.

The following discussion is divided into two sections. Section 3.1 focuses on the effects of the symmetry breaking in the lateral dimension (perpendicular to the sliding direction) and its effect on the shape of plots of the system prop-

erties as a function of unit-cell distance. System properties relating to the sliding and compressing directions exhibit an approximate periodicity over a half-unit cell. Section 3.3 focuses on this approximate periodicity. The trends here are those that are most important in understanding the properties of a system that will extend more generally to counter-surface probes whose geometry is not commensurate with the underlying substrate.

3.1. The lateral dimension: breaking of symmetry

Figure 1(b) shows a snapshot of the lateral dimension of the system during the sliding phase. There are two possible configurations that the chains can adopt: a right-handed orientation in which a chain will circulate counterclockwise starting from the bottom, and a left-handed orientation where a chain circulates clockwise. During equilibration and compression, chains adopt either a right-handed or left-handed configuration (figure 2). It appears that the handedness of the chains are correlated because most of the chains in the center region share the same configuration. However, not all the chains share the same handedness. While there is

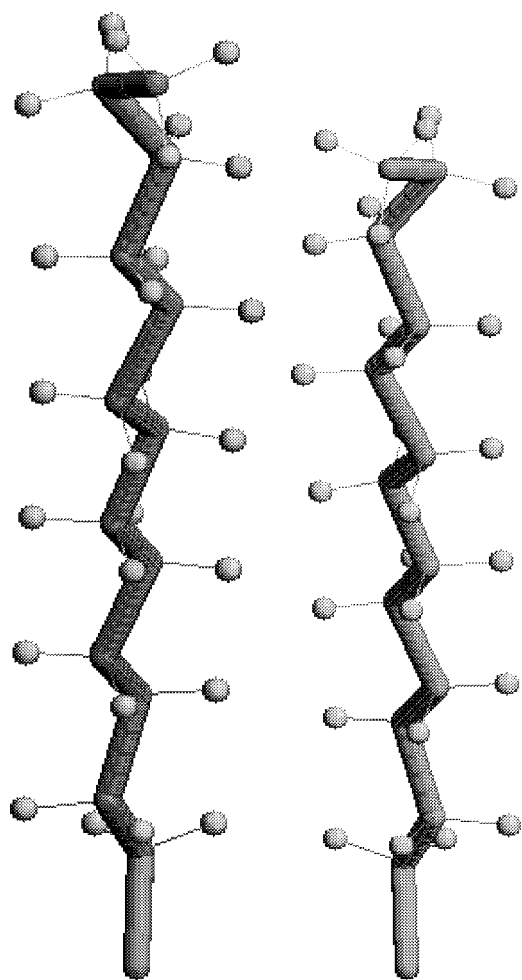


Figure 2. The chain on the left has a left-handed orientation (the carbon backbone circulates clockwise starting from the bottom), while the chain on the right shows a right-handed orientation.

an obvious random component associated with how chains choose a particular handedness, analysis reveals that none of the chains change their orientation during sliding.

A possible explanation of this asymmetry is that the indentation speed of the counterface is too fast to allow all chains to adopt the same handedness; some become pinned before they can adjust to their neighbors. Given that there are only 36 chains, this may imply that similarly prepared systems could easily exhibit large differences in their relative numbers of gauche defects after compression owing to the partially random manner in which the chains choose handedness under compression. This suggests that compression of the monolayer results in a fixing of the handedness of the chains. It will be important to assess how this fixing of handedness is related to other system properties such as the number of gauche defects, temperature, and indentation speed.

The breaking of symmetry during the compression of the monolayer is also evident in the top panel of figure 3, which shows the azimuthal angle ϕ as a function of sliding distance. This angle is taken to be the angle between the sliding direction and the projection of the carbon backbone in the plane that contains the monolayer. It is calculated by averaging over all possible angles defined by alternating carbons along the backbones of the chains. This angle shows the chains getting pushed from side to side as each wave of the hydrogen atoms of the counterface pass by with the frequency of a half-unit cell. Unlike the case of handedness where both types are adopted, an animated sequence of the carbon backbones of the chains, viewed from above the chains, shows that the side to side motion of the chains is completely correlated. All chains move to the same side in a synchronized motion. The motion is not symmetric about zero (though it does pass through zero); this shows

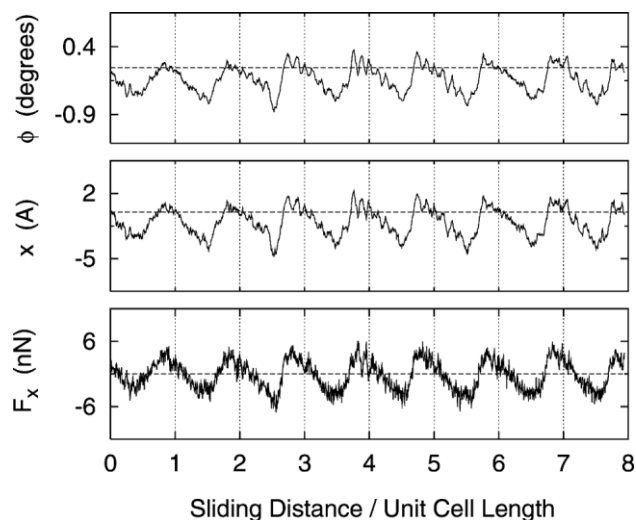


Figure 3. Lateral direction: average force F_x on the countersurface in the x direction, average x coordinate of the top carbon atoms in the alkane chains, and azimuth angle ϕ as a function of the sliding distance. (More complete definitions can be found in the text.) The sliding distance has been divided by the unit cell length that corresponds to the (2×2) packing of the chains.

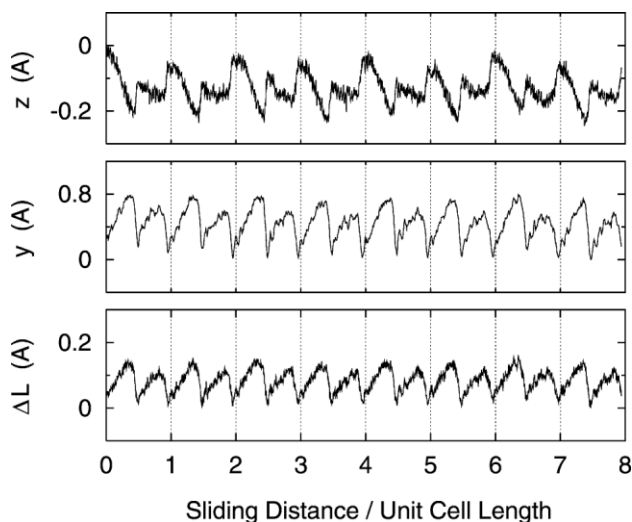


Figure 4. Sliding direction: average displacement of the carbon-carbon bonds in the alkane chains ΔL and average y and z coordinates of the top carbon atoms in the alkane chains as a function of the dimensionless sliding quantity described in figure 3.

the chains are preferentially shifted to one side. Thus, it is only after sliding through one unit cell that the chains return to the starting geometry. This periodicity is also observed in the average lateral trajectory of the top carbon atoms of the monolayer x (figure 3) and in the lateral force exerted by the counterface F_x (figure 3) as functions of the sliding distance.

As with the choice of handedness, prior to compression there is no preferential side for the chains to be pushed. It would be interesting to establish if the choice of handedness and azimuthal bias are correlated. This would require the investigation of friction for a number monolayer starting configurations that had random orientations. (This is accomplished via the use of different random number seeds in the MD simulation.) The effect of this asymmetry in azimuthal angle is that the chains adopt a slightly different geometry over the half-unit cell. In one extreme, the tops of the chains are laterally closer to the anchored bottom of the chains; in the other extreme they are farther apart. Similarly, the tops of the chains alternate over the half-unit cell between positions far from the counterface hydrogen atoms or close to them in the lateral direction. This leads to the different peak shapes in properties associated with the sliding and loading directions (figures 4 and 5). In other words, while there is an approximate periodicity in these properties associated with a half-unit cell (each wave of counterface hydrogen atoms), this periodicity is modified by the close/far asymmetry in the lateral direction.

One final comment with regard to the lateral dimension, it is interesting to note that all the lateral dimension plots of figure 3 exhibit a startup sliding effect. The final shape of the period oscillation is achieved after two or three unit cells. This is likely due to the fact that the slide starts with the counterface at rest, it takes a few unit cells for the monolayer to achieve a steady state. It may also be possible that the initial sliding allows for some settling of the disorder caused by the randomness associated with the compression

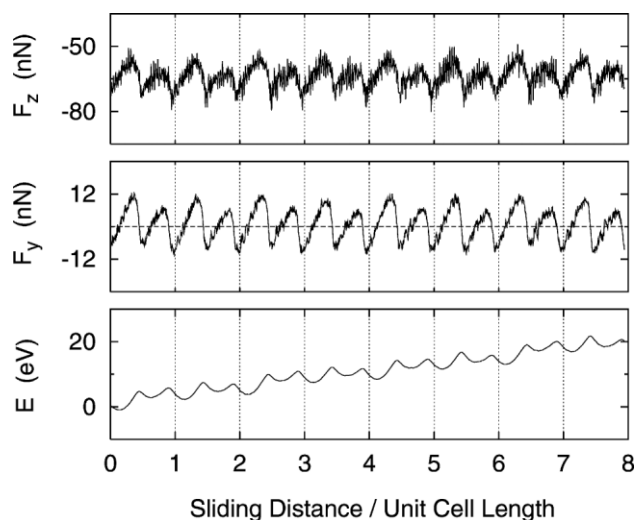


Figure 5. Sliding direction: average system energy E and average friction F_y and normal F_z forces on the countersurface as a function of the dimensionless sliding quantity described in figure 3.

of the monolayer. In either case, this implies it is best to conduct any quantitative analysis far from any abrupt transition region.

3.2. The sliding and loading directions: approximate periodicities

The approximate periodicity associated with the movement through a half-unit cell is easily seen by observing the trajectory of the carbon atom at the end of a chain. Figure 4 shows this trajectory, averaged over all chains, for the compression (y) and the sliding (z) directions. Each wave of hydrogen atoms from the counterface interacts with the top of the chain, slightly compressing and stretching the chains. When the counterface hydrogen atoms pass over the top of the chains, the chains spring back to the uncompressed, unstretched state. The chains are then caught by the next wave of hydrogen atoms and the process is repeated.

The stretching out in the sliding direction is not confined to the ends of the chains: it extends throughout the entire chain. This is apparent from examination of the average change in length along the chain backbone, ΔL (figure 4) versus sliding distance. (This quantity follows the backbone along consecutive carbon atoms. Thus, it is twelve times the average bond length between carbons in the chains.) This is only one representative quantity. Other quantities that can accommodate a stretching of the chain include the angle defined by three successive carbons, the gauche angle, as well as the analogous distances associated with these angles. The stretching of the chains is also linked with a slight increase in the tilt angle.

During the spring back phase, the friction force F_y changes sign as the chains push the counterface hydrogen atoms (figure 5). It is important to note that the fluctuations in the friction force are significantly larger than the average force. The implication being that while the motion of the counterface on the whole is steadily depositing energy

into the system (slope of E in figure 5), at any given instant it can either be depositing or removing energy to this system depending on whether it is pushing the chains or being pushed by them. This is evident in figure 5, which shows the total energy of the system E . While this quantity is calculated by summing the kinetic and potential energies plus the work done on the bath, it is equivalently the integral of the frictional force over the sliding distance.

The periodicity associated with F_y is very regular. This implies that the channels for energy dissipation associated with this force should similarly exhibit this extremely regular periodic behavior. While the geometrical features discussed above are tightly correlated with the friction force, it is not clear what role these and other features play in the dissipation of energy. Previous studies have correlated the formation of gauche defects with friction force [27], but have not quantitatively connected this process to the energy of the system. A quantitative analysis of monolayer features and their relative roles in energy dissipation is currently under investigation [39].

4. Future work

The above strongly suggests that the frictional properties associated with sliding of a diamond counterface over a tightly packed SAM possessing a commensurate geometry can be understood in terms of the collective synchronized motions of the chains. The usefulness of these kinds of monolayers as a nanolubricant is probably related to this property. In a sense, the ability to maintain a regular periodic geometry yet at the same time be fairly mobile make the monolayer both solid-like and liquid-like. It is tempting to entertain the possibility that these are the two essential qualities of SAM systems. This hypothesis can be tested simply by repeating these simulations with fewer chains and smaller periodic boundary conditions. In fact, one might be tempted to simply use a single unit cell.

If the simple system implies the same liquid-like and solid-like properties observed here, there are a host of interesting possibilities to investigate. With a system so small, present computational resources would allow for the simulation to be conducted at slower speeds and for much longer times. A reasonable approach might be to conduct the simulation in a simultaneous indenting and sliding mode (including the equilibration phase). By keeping the indentation speed much smaller than the sliding speed, the entire simulation can be run without any abrupt transitions. Without transition periods, a realistic estimate of the frictional force for a given load is achieved by averaging the slide over one unit cell because there are no start-up effects. Over such a short distance, the indentation speed can be made slow enough such that the change in the load due to the indentation is not of great importance. The result is the construction of a precise friction versus load curve, something previously only simulated for a few points.

This economical approach could be used to investigate a number of things, such as the effects of chain length, sliding

direction, offset of the counterface, and compression speed, and sliding speed on system properties. More limited simulations can similarly be conducted on somewhat larger systems to help quantify the effects of disorder within the monolayer. It is possible that temperature and speed effects will be the most dramatic. The artificially ordered one-chain system may provide a useful baseline against which effects of disorder can be assessed. While obviously limited in some respects, this baseline system is an interesting avenue to explore because it can be conducted at a scale that is orders of magnitude different from present simulations.

Acknowledgement

This work was supported by the US Office of Naval Research (ONR) under contract N00014-00-WR-20186 and in part by the Air Force Office of Scientific Research (AFOSR) under contract NMIPR-00-5203503.

References

- [1] A.M. Homola, C.M. Mate and G.B. Street, *MRS Bulletin* 15 (1990) 45.
- [2] S.S. Perry, G.A. Somorjai, C.M. Mate and R.L. White, *Tribol. Lett.* 1 (1995) 233.
- [3] S.S. Perry, G.A. Somorjai, C.M. Mate and R. White, *Tribol. Lett.* 1 (1995) 47.
- [4] V.V. Tsukruk et al., *Tribology Issues and Opportunities in MEMS* (Kluwer Academic, Dordrecht, 1998) pp. 607–614.
- [5] K. Deng, R.J. Collins, M. Mehregany and C.N. Sukenik, *J. Electrochem. Soc.* 142 (1995) 1278.
- [6] H.I. Kim, M. Graupe, O. Oloba, T. Doini, S. Imaduddin, T.R. Lee and S.S. Perry, *Langmuir* 15 (1999) 3179.
- [7] A. Lio, C. Morant, D.F. Ogletree and M. Salmeron, *J. Phys. Chem. B* 101 (1997) 4767.
- [8] R.W. Carpick and M. Salmeron, *Chem. Rev.* 97 (1997) 1163, and references therein.
- [9] A. Lio, D.H. Charych and M. Salmeron, *J. Phys. Chem. B* 101 (1997) 3800.
- [10] H.I. Kim, T. Koini, T.R. Lee and S.S. Perry, *Langmuir* 13 (1997) 7192.
- [11] X. Xiao, J. Hu, D.H. Charych and M. Salmeron, *Langmuir* 12 (1996) 235.
- [12] J.A. Harrison and S.S. Perry, *MRS Bulletin* 23 (1998) 27.
- [13] S. Lee, Y.-S. Shon, R. Colorado, R.L. Guenard, T.R. Lee and S.S. Perry, *Langmuir* 16 (2000) 2220.
- [14] E. Barrena, S. Kopta, D.F. Ogletree, D.H. Charych and M. Salmeron, *Phys. Rev. Lett.* 82 (1999) 2880.
- [15] A.R. Burns, J.E. Houston, R.W. Carpick and T.A. Michalske, *Phys. Rev. Lett.* 82 (1999) 1181.
- [16] W. Mar and M.L. Klein, *Langmuir* 10 (1994) 188.
- [17] R. Bhatia and B.J. Garrison, *Langmuir* 13 (1997) 765.
- [18] R. Bhatia and B.J. Garrison, *Langmuir* 13 (1997) 4038.
- [19] W.D. Luedtke and U. Landman, *J. Phys. Chem.* 102 (1998) 6566.
- [20] K.J. Tupper, R.J. Colton and D.W. Brenner, *Langmuir* 10 (1994) 2041.
- [21] K.J. Tupper and D.W. Brenner, *Langmuir* 10 (1994) 2335.
- [22] J.N. Glosli and G.M. McClelland, *Phys. Rev. Lett.* 70 (1993) 1960.
- [23] T. Ohzono, J.N. Glosli and M. Fujihira, *Jpn. J. Appl. Phys.* 37 (1998) 6535.
- [24] M. Fujihira and T. Ohzono, *Jpn. J. Appl. Phys.* 38 (1999) 3918.
- [25] A. Koike and M. Yoneya, *Langmuir* 13 (1997) 1718.
- [26] T. Bonner and A. Baratoff, *Surf. Sci.* 377–379 (1997) 1082.
- [27] A.B. Tutein, S.J. Stuart and J.A. Harrison, *Langmuir* 16 (2000) 291.

- [28] J.A. Harrison, P.T. Mikulski, S.J. Stuart and A.B. Tutein, *Nanotribology: Critical Assessment and Research Needs* (Kluwer Academic, Norwell, MA, 2000).
- [29] A.B. Tutein, S.J. Stuart and J.A. Harrison, *J. Phys. Chem. B* 103 (1999) 11357.
- [30] S.J. Stuart, A.B. Tutein and J.A. Harrison, *J. Chem. Phys.* 112 (2000) 6472.
- [31] P. Fenter et al., *Science* 266 (1994) 1216.
- [32] S.A. Adelman and J.D. Doll, *J. Chem. Phys.* 64 (1976) 2375.
- [33] W.C. Swope, H.C. Andersen, P.H. Berens and K.R. Wilson, *J. Chem. Phys.* 76 (1982) 637.
- [34] D.W. Brenner, *Phys. Rev. B* 42 (1990) 9458.
- [35] D.W. Brenner, J.A. Harrison, R.J. Colton and C.T. White, *Thin Solid Films* 206 (1991) 220.
- [36] B.J. Garrison, E.J. Dawnkaski, D. Srivastava and D.W. Brenner, *Science* 255 (1992) 835.
- [37] J.A. Harrison and D.W. Brenner, *J. Am. Chem. Soc.* 116 (1994) 10399.
- [38] J.A. Harrison, S.J. Stuart and M.D. Perry, *Tribology Issues and Opportunities in MEMS* (Kluwer Academic, Dordrecht, 1998) pp. 285–299.
- [39] P.T. Mikulski and J.A. Harrison, in preparation.